Effect of recirculation and hydraulic loading rate on ammonium and phosphate recovery from fertilizer industry wastewater

I Dewa Ayu Agung Warmadewanthi [a,*], Nurani Ikhlas [b], Febrianda Damayanti [a]

[a] Department of Environmental Engineering, Faculty of Civil, Environmental, And Geo-Engineering, Institut Teknologi Sepuluh Nopember, Kampus ITS Sukolilo, Surabaya, 60111, Indonesia
[b] Environmental Sustainability Research Group (ENSI-RG), Department of Environmental Engineering, Faculty of Engineering, Universitas Diponegoro, Semarang, 50275, Indonesia

A B S T R A C T

This study aimed to determine the optimum recirculation ratio and hydraulic loading rate for the recovery process of ammonium and phosphate, and study the formation, morphology, and structure of struvite crystals. This study provides a crystallization method to treat fertilizer wastewater using a continuous system and recirculation, including a fluidized bed reactor (FBR). Ammonium and phosphate were recovered from fertilizer industry wastewater using a continuous FBR under different recirculation ratios (3, 6, and 9) and loading rates (0.39 L/min, 0.59 L/min, and 0.79 L/min). $MgCl_2$ was used as the precipitant with a 1.5:1 molarity ratio $[Mg^{2+}]:[PO_4^{3-}]$. The results showed that 55.71% phosphate and 49.69% ammonium could be recovered at recirculation ratio and hydraulic loading rate were 9 and 0.39 L/min, respectively. Scanning electron microscopy-energy diffraction X-ray analysis showed that the formed crystals comprised 80% struvite. Further, a high recirculation ratio and low loading rate resulted in higher ammonium and phosphate recovery efficiencies. These results indicated that a long detention time of treated wastewater can increase the nutrient recovery.

1. Introduction

Fertilizer wastewater commonly contains high concentrations of phosphate and ammonium [1,2], fluoride [3], heavy metals, and suspended solids [1]. These high ammonium and phosphate concentrations can cause eutrophication [4,5]. Many studies on phosphate recovery have been conducted because the availability of phosphate can dissipate in the future. Approximately 90% of the phosphate is derived from non-renewable phosphate rocks. The availability of phosphate will last only for the next 100 years [6,7]. The non-renewable nature of phosphate rocks has led to increased ongoing research on phosphate recovery [8]. Wastewater treatment, which involves phosphate recovery, is an alternative source of renewable phosphate.

Wastewater treatment from the fertilizer industry using phosphate and ammonium recovery processes has shown great potential for producing products with high application value as slow-release fertilizers and products with a low degree of impurities [1,4,9,10]. Slow-release fertilizers can be formed at appropriate concentrations of magnesium, ammonium, and phosphate using a crystallization or precipitation process [10], biological degradation, crystallization, tertiary filtration, and ion exchange [1], electrodialytic recovery

of ammonium and phosphate ions using a continuous-flow reactor [11], using gypsum waste [12], and struvite crystallization with DTM (*Draft Tube Magma*) type constructions [13]. The crystallization or precipitation process produces a reusable crystal as a slow-release fertilizer called struvite [14].

During the chemical precipitation process, the resulting phosphate is bound as a compound in the sludge, with a removal percentage of 70%–95%. The crystallization process differs from that of chemical precipitation, in which the resulting phosphate comprises reusable crystals [5,14,15]. Crystallization can remove 80%–90% phosphate [6]. The disadvantages of chemical precipitation include an increase in ammonium caused by adding coagulants and the formation of compounds that can corrode processing units [16]. Li et al. Shim et al., and Zhang et al. reported that this results in a high recovery rate and excellent economic efficiency during crystallization [14,15,17].

The crystallization of magnesium and phosphate can produce three products, namely newberryite ($MgHPO_4 \cdot 3H_2O$), trimagnesium phosphate ($Mg_3(PO_4)_2 \cdot 22H_2O$), and bobierrite ($Mg_3(PO_4)_2 \cdot 8H_2O$). Struvite ($MgNH_4PO_4 \cdot 6H_2O$) can also be produced with appropriate concentrations of magnesium, ammonium, and phosphate [18]. Struvite recovered from fertilizer wastewater is a sustainable option for phosphate recovery and fertilization [19]. Sustainable development and environmental preservation through production recovery purposes to use wastes as another potential in the form slow-release fertilizers low metal content compared with those released from phosphate rocks [15,20]. Factors that affect the phosphate crystallization process include pH [5], molar ratio of Mg^{2+}, NH_4^+, and PO_4^{3-} [15], ion content in impurities [21,22], recirculation, and the precipitant used [14].

Several studies have reported results on the recovery of ammonium and phosphate from fertilizer wastewater using a batch system reactor with $MgCl_2$ having a 99% phosphate removal rate [2]. Warmadewanthi et al. reported that the optimum molar ratio of $[Mg^{2+}]$: $[NH_4^+]$:$[PO_4^{3-}]$ was 1:1:1 [18]. The use of a fluidized bed reactor (FBR) has proven to be superior because it can achieve a phosphate recovery rate of up to 91% [17]. FBR is also reported to be more superior compared to conventional precipitation methods [15,17,23]. A continuous stirring tank reactor (CSTR) of the FBR can only recover up to 80–85% phosphate. Therefore, the use of continuous system in the laboratory mode can provide a better insights for real life application [24]. The addition of a recirculation process can also increase the minimum theoretical equivalent diameter, which can in turn increase the heterogeneous nucleation and crystal growth [18]. Using a continuous FBR with a recirculation process can affect the hydraulic loading rate of the influent, thereby changing the flow rate drastically. Increasing the flow rate consequently leads to a higher mass transfer and larger crystal sizes. Therefore, the flow rate must be controlled to maintain the hydraulic loading rate [22]. This research provides a crystallization method, which differs from that used previously, to treat fertilizer wastewater using a continuous system and recirculation, including a CSTR and FBR. Particularly, this study aimed to determine the optimum influent recirculation ratio and hydraulic loading rate for phosphate and ammonium recovery using an FBR. A fertilizer industry was the source of fertilizer wastewater, which was high in phosphate and ammonium contents [18].

2. Calculation

Fluidization occurs when the fluid velocity through the solid is equal to the gravity of the solids and the particle drag [25]. The minimum fluidization speed was calculated using Equations (1)–(3), and the maximum fluidization speed was calculated according to Equations (4) and (5) as follows:

$$\upsilon mf = \frac{(\psi dp)^2}{150\mu} \text{ x } \eta \text{ x } \left(\frac{\epsilon mf^2}{1 - \epsilon mf} \right) \tag{1}$$

$$\epsilon mf = 0,586 \times \psi^{-0.72} \times \left(\frac{\mu^2}{\rho f \times \eta \times dp^3} \right)^{0.029} \times \left(\frac{\rho f}{\rho b} \right)^{0.021} \tag{2}$$

$$\eta = g(\rho b - \rho f) \tag{3}$$

where υmf is the minimum fluidization speed (m/s), ψ is the sphericity or shape factor, dp is the average particle diameter (m), μ is the kinematic fluid viscosity (kg.m/s), g is the specific gravity (m/s^2), ρb is the bed density (kg/m^3), ρf is the fluid density, ϵmf is the void fraction at minimum fluidization, and Re is Reynolds number. The maximum fluidization velocity (υt) occurs when the fluid velocity is overestimated. The particles followed the fluid flow in the bed. Maximum fluidization velocity occurs when the upward force exceeds the gravitational force [25].

When Re < 0.4,

$$\upsilon t = \text{x} \frac{dp^2}{18} \mu \tag{4}$$

when 0.4 < Re < 500,

$$\upsilon t = \left(1,78 \text{ x } 10^{-2} \text{ x } \frac{\eta^{-2}}{\rho f} \text{ x } \mu \right)^{\frac{1}{3}} \text{ x } dp \tag{5}$$

According to Equations (1)–(5), the velocity for each recirculation ratio can be calculated. The flow velocity in this study was in the range of υmf and υt values of each recirculation ratio. The flow velocity was regulated using a pump to determine the flow rate or hydraulic loading rate in the reactor using Equation (6) [9].

$$Q_m = A \text{ x } υmf \tag{6}$$

where Q_m is the flow rate or hydraulic loading rate (m^3/s), A is the reactor area (m^2), and υmf is the minimum fluidization speed (m/s).

In struvite crystals, the theoretical molar ratio of nitrogen, phosphorus, and magnesium was 1.5:1. The magnesium ions in struvite crystals can form other crystals, such as magnesium phosphate or magnesium hydrogen phosphate. Accordingly, in the obtained crystals, every 1 mol of ammonia nitrogen could be regarded as 1 mol of struvite [23]. The purity of struvite based on the recovery results was calculated using Equation (7) [26].

$$Purity \text{ of } struvite = \frac{n_{NMstruvite}}{m_{Product}} x \text{ } 100\% \tag{7}$$

where n_N is the mole of NH4–N, $M_{struvite}$ is the molar mass of struvite, and $m_{Product}$ is the product mass.

3. Material and methods

3.1. Sample collection

Samples were collected from fertilizer industry wastewater treatment plant (WTP). The WTP unit consisted of an equalization tank and a settling pond. Wastewater samples (35 L) were collected three times a day using a composite sampling technique is a mixture of several samples taken at the same point but at different times. In this study, samples will be taken in the morning (8 a.m.), afternoon (11 a.m.), and evening (2 p.m.). The collected samples will be composited to obtain 105 L of composite samples. Sample preservation in this research parameter test is adjusted to the standard method. That is, a mixture of several samples was collected at the same point but at different times. Samples were collected to obtain 105 L of composite samples. The chemical composition of the fertilizer wastewater is presented in Table 1. Samples were preserved according to the standard methods for further parameter tests.

3.2. Experimental setup and procedures

This study used an FBR consisting of two parts: a lower part (height: 1.5 m, diameter: 0.05 m), where crystallization reaction occurred, and a top part (height: 0.25 m, diameter: 0.1 m), which functioned as a crystal catcher to ensure that no crystals were carried into the effluent bath or freeboard. The FBR was designed using a recirculation process by flowing the wastewater three, six, and nine times. The recirculation ratios were 3, 6, and 9, and the hydraulic loading rates were 0.39 L/min, 0.59 L/min, and 0.79 L/min. The determination of recirculation ratio and hydraulic loading rate were based on the Seckler and Le Corre et al. methodology which highlighted the value of optimum recirculation ratio and hydraulic loading rate on crystallization process [27,28].

In the early stages of the study, the molar ratio of [Mg^{2+}]:[PO$_4^3$] was determined to reach 1.5:1 after adding MgCl$_2$·6H$_2$O (Merck, Germany). Ikhlas and Warmadewanthi reported that the precipitant of MgCl$_2$ was optimal for recovering phosphate and ammonium from fertilizer wastewater. Subsequently, the pH of the solution was adjusted to a range of 8.5 ± 0.2 [2]. The influence of crystallization was controlled by maintaining the working pH in the alkaline range of 8–9.5 [29]. Adjustments can be made by adding a strong base, such as NaOH (Merck, Germany), or a strong acid, such as H$_2$SO$_4$ (Merck, Germany), at a dose calculated based on the neutralization requirements. Crystal composition was used to determine the FBR productivity. Analyses of the morphology and crystal structure determined the optimum crystal quality.

The reactor comprised two compartments. In the first compartment, the crystallization reaction of phosphate and ammonium occurred. The second compartment functioned as a freeboard and crystal catcher. There were two inlets leading to the reactor: one to the wastewater basin and the other for MgCl$_2$. The wastewater tank contained a mixture of wastewater from fertilizer industry. Its pH had been conditioned to the optimum reaction pH by adding NaOH or H$_2$SO$_4$ solutions. The wastewater tank also included wastewater from recirculation. The MgCl$_2$ bath contained MgCl$_2$ dissolved in water.

Table 1
Characteristics of fertilizer wastewater.

Parameters	Concentration	Analytical method
pH	8.63	pH meter (BP3001, Trans Instrument, Singapore)
Magnesium (mg/L)	312.9	Spectrophotometer [42]
Phosphate (mg/L)	1800	Spectrophotometer [42]
Ammonium (mg/L)	1710	Spectrophotometer [42]
Fluoride (mg/L)	122	Spectrophotometer [42]
TSS (mg/L)	122.22	Gravimeter [42]
Chemical oxygen demand (mg/L)	72	Reflux [42]
Silica (mg/L)	850	Spectrophotometer [42]
Calcium (mg/L)	101.2	Spectrophotometer [42]

The working mechanism of the reactor involved pumping wastewater from the wastewater basin to the reactor using a diaphragm pump (Fig. 1). Simultaneously, $MgCl_2$ solution was pumped into the reactor using a diaphragm pump. The diaphragm pumps were equipped with discharge settings and flow meters. The volume of water pumped from the influent and $MgCl_2$ tubs had a ratio of 1:1 [23,29]. Before entering the reactor, the wastewater passed through a flow meter or discharge-measuring device. In Chamber 1, a pressure gauge was present, which indicated when the minimum and maximum fluidization velocities and clogging were achieved. When the treated water reached the top of the reactor, it flowed into the effluent pipe.

Wastewater from the effluent pipe was then recirculated into the reactor. The repetition was performed with as many variations as possible for a specified recirculation. Before the wastewater entered the reactor, a recirculating stream was used to check the phosphate, ammonium, and magnesium contents to determine the mass balance of the reaction. Sampling was performed at every recirculation turn. After passing the recirculation limit, the wastewater from the effluent flowed into the effluent tub by closing the valve in the recirculation pipe. In the effluent bath, the wastewater content was checked at a time interval of 2.5 min for induction and 10 min for reaction.

This study determined the fluidization velocity of the recirculation process using water and sand media to suspend the solid particles and cause the solids to behave as fluids [30]. The sand media consisted of particles of sizes 100, 200, and 400 μm for recirculation ratios of 3, 6, and 9. The experiment was conducted by placing the sand media in the reactor. Water flowed into the reactor through the sand media until fluidization occurred. The calculated minimum and maximum fluidization speeds were adjusted to the field conditions. Further, the theoretical calculations of the minimum and maximum fluidization velocities were verified under field conditions. The induction time was determined to have the highest variation in the recirculation ratio and a high hydraulic loading rate. Nucleation takes more time in these variations, and thus, the reaction time was also long [31]. The induction and operating time data were obtained by decreasing the phosphate and ammonium concentrations in the effluent and the clogging time.

3.3. Analytical methods

The morphologies, structures, and compositions of the crystals were investigated. The composition of the crystals was used to determine the productivity of the FBR. Before analysis, the sample was coated to enhance its conductivity and clearly present the resulting image. Before examination, the samples were dried in a desiccator for 48 h. Samples were examined at 100x and 1000x
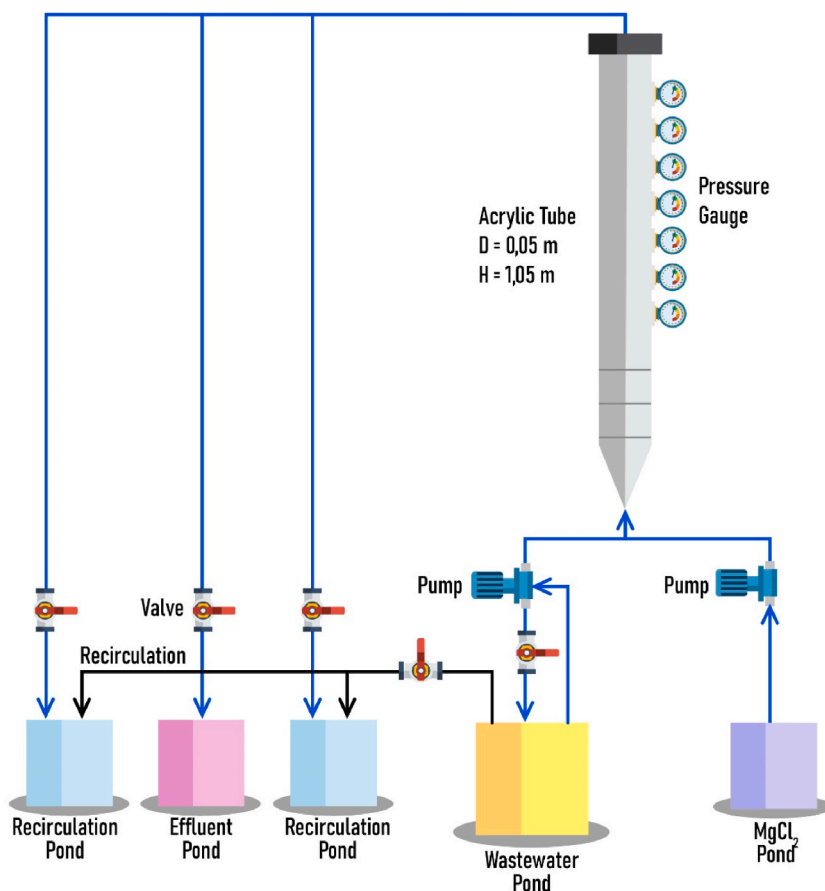

Fig. 1. Schematic diagram of wastewater flow.

magnifications. The morphologies and structures of the formed crystals were examined to determine their quality, using scanning electron microscopy-energy diffraction X-ray (SEM-EDX) method. The particle size distribution and crystal composition were determined by wet analysis and X-ray diffraction (XRD). The results of this XRD investigation were then processed using the application "Match! Phase Identification from Powder Diffraction" version 3.6.2.121. The application analyzed the substance composition based on the intensity of the peak point reflected at the sample.

4. Results and discussion

4.1. Recovery of phosphate and ammonium

In this study, recirculation ratios of 3, 6, and 9 were used to determine the optimum recirculation ratios at hydraulic loading rates of 0.39, 0.59, and 0.79 L/min. Recirculation could increase the phosphate removal efficiency because of the homogeneous nucleation process in the reactor. Therefore, the optimum recirculation ratio of the crystallization process was 2–9, with a hydraulic loading rate of 400–410 cm/h [21]. The phosphate removal efficiency reached 85% in this recirculation ratio range. If it exceeds this range, the removal efficiency would be the same as that without recirculation. Increasing the recirculation flow can also increase the minimum diameter of the formed crystals [23]. Heterogeneous nucleation occurred between the particles formed during recirculation and those in the basin. Liu et al. mentioned that heterogeneous nucleation occurs in the reactor on a small level; thus, homogeneous nucleation during recirculation increased, and the crystals formed became purer [32].

The phosphate and ammonium recovery efficiencies showed that the phosphate concentration decreased drastically after recirculation and remained relatively constant until the next operation. These results indicated that during recirculation, homogeneous nucleation occurred in the reactor [32]. Homogeneous nucleation indicates the formation of crystal nuclei in the reactor. Termination of homogeneous nucleation follows discontinuation of the recirculation process. Secondary nucleation then occurs, wherein the crystal diameter enlarges due to contact between the elements in the wastewater and the crystal nuclei in the reactor. Moreover, the duration of the secondary nucleation process indicates the size of the crystals formed [33].

As shown in Table 2, increasing the recirculation ratio in an FBR can increase phosphate and ammonium removal [21]. Warmadewanthi and Bachtiar reported that decreasing the hydraulic loading rate to 1.2 L/min would reduce phosphate and ammonium removal by 1% [22]. The hydraulic loading rates of 0.39, 0.59, and 0.79 L/min of phosphate removal without recirculation were 48.4%, 48.5%, and 48.62%, respectively. The recirculation ratio of 9 increased the removal efficiency by 7.31%, 2.4%, and 1.19% at hydraulic loading rates of 0.39 L/min, 0.59 L/min, and 0.79 L/min, respectively. Moreover, recirculation ratios 3 and 6 resulted in reduced efficiency. The highest removal efficiencies were 6.04% and 2.95% at hydraulic loading rates of 0.39 L/min and 0.59 L/min, respectively. The highest ammonium removal efficiency was reported at a recirculation ratio of 9 and a hydraulic loading rate of 0.39 L/min; particularly, the ammonium removal efficiency increased by 6.62% and 1.40% at a hydraulic loading rate of 0.59 L/min. The optimum recirculation ratio that can be used was 9 because it could increase phosphate and ammonium recoveries. Table 2 shows that for every increase in the hydraulic loading rate by 0.20 L/min for a recirculation ratio of 9, the percentage of phosphate recovery decreased by 1–5%. A decrease in the hydraulic loading rate by 0.20 L/min at a recirculation ratio of 6 reduced the phosphate removal efficiency by 2–3%. Therefore, the optimal hydraulic loading rate was 0.39 L/min. The increased hydraulic loading rate can decrease the induction time. The optimum hydraulic loading rate based on induction time is 0.39 L/min for all recirculation ratios. The higher the detention time of wastewater in the reactor, the greater the efficiency of phosphate recovery. The longer wastewater detention time in the reactor, the absorption of phosphate content for crystal formation has already occurred ideally before the wastewater reaches the effluent. The size of the formed crystals will increase with longer reaction times without using seed material by controlling the hydraulic loading rate [31].

Regarding each recirculation ratio with a hydraulic loading rate variation of 0.79 L/min, the ammonium removal was not greater than that without recirculation. This occurred because the formed particles were too small; therefore, the density of the particles formed was low. Further, the particles with low density were fluidized at high speed; therefore, more particles were formed in the effluent basin, which was consistent with the findings of Tarragó et al. [21]. The percentage of ammonium recovery was lower because the atomic weight of ammonium is lower than that of phosphate [31]. Hence, the mass of struvite-forming ammonium was less than that of phosphate [34].

Table 2
Efficiency recovery of phosphate and ammonium.

Hydraulic loading rate	Phosphate			Ammonium		
	Recirculation ratio					
	3	6	9	3	6	9
0.39 L/min	48.09%	48.80%	55.71%	45.51%	46.06%	49.96%
0.59 L/min	47.22%	48.63%	50.90%	42.69%	43.06%	44.90%
0.79 L/min	46.52%	48.40%	49.81%	40.31%	40.70%	41.50%

4.2. Effect on pH

At initial condition, the average pH value during the crystallization process in the fluidized bed reactor was set to 8.5 ± 0.2. This pH value is obtained without adding NaOH or H_2SO_4 to the reactor during the process. At the end of recirculation, the pH value decreased. The loss of carbonate ions decreases the pH of the wastewater. The pH value then increased at the end of recirculation. This was due to a decrease in the maximum solubility of the crystals formed [35]. At recirculation ratios of 3 and 9, there was a difference in the increase in pH at the end of the process. At a recirculation ratio of 9, the pH value was stable, while at a recirculation ratio of 3, the pH value increased at the end of the process. This was believed to be due to the remaining alkalinity of bicarbonate ions in the water, which decreased the percentage of phosphate removal [36]. Alkalinity also plays an essential role in phosphate removal. Alkalinity can reduce the phosphate removal efficiency during struvite precipitation [23,36]. Additionally, an increase in pH can increase super-saturation and fluctuate the percentage recovery. High supersaturation levels can affect the crystallization process in FBR [21,36]. pH is an essential factor in struvite formation as it affects the solubility of struvite and its thermodynamic properties [16]. Moreover, high pH values can enhance the nucleation rate of struvite crystals [35]. However, when the pH reaches its optimum value (pH precipi-tation), the pH of the solution decreases. This was due to the simultaneous release of protons in the solution with struvite precipitation [23]. The pH values observed in this study during crystallization are shown in Fig. 2(A-C).

4.3. Effect on total suspended solids (TSS) concentrations

The results showed that the particle size decreased with lower temperature under otherwise constant conditions and reached a minimum value between pH 9 and 10. Deviating trends were observed at pH < 8. Struvite formation in a CSTR was a reliable and stable process that did not require pH control. A method based on conductivity measurements was presented to estimate the ionic strength, which was required to maintain equilibrium so that the refined particles in the wastewater support the nucleation process in the reactor. Heterogeneous nucleation occurred during particle recirculation in wastewater treatment plant. Therefore, the heterogeneous nucleation process in the reactor was significantly reduced. Subsequently, this increased homogeneous nucleation during recirculation (Table 3).

The optimum recirculation ratio and hydraulic loading rate can eliminate the highest amount of TSS, as reported by Ronteltap et al. [16]. Struvite crystallization is a fast and reliable phosphorus removal and recovery process for concentrated waste streams, such as hydrolyzed human urine. To optimize the phosphorous removal efficiency, larger particle sizes can be obtained because they are easier to separate and less prone to washing out than smaller particles. Crystals formed in batch experiments with real hydrolyzed urine were shown to have an average size of >90 mm at pH 9 and 20 °C. Moreover, the crystal size was reduced to 45 mm when the type of stirrer was changed.

### 4.4. Characterization of crystals

As shown in Fig. 3, the crystal shape resembled a cube, as mentioned in a previous study [15]. The crystal surface has various small holes and cracks caused by incomplete crystallization and the presence of impurity ions that interfere with the crystallization process [23,27]. As seen in Fig. 3(A), the crystals formed at a recirculation ratio of 9 resembled elongated cubes. The shapes of the observed precipitates resembled those of struvite crystals. On the surface of the formed crystals, a small proportion of precipitate sticks and holes were observed. This was because the impurity ions reacted with struvite. Reactive impurity ions include silica, fluorine, and calcium [35].

Further, as shown in Fig. 3(B), the crystals formed were almost identical to those formed at a recirculation ratio of 9. However, the diameter of the crystals formed was much larger at this ratio. This corresponded to the theory of the recirculation process that the greater is scale of the recirculation process, the greater the diameter of the resulting crystal [23,35,37]. Moreover, at a recirculation ratio of 6, the crystals had more holes than in the crystals that precipitated. This was due to the interference from dominant fluoride ions.

The XRD analysis results (Fig. 4(A)) showed that the optimum hydraulic loading rate and recirculation ratios were 0.39 L/min and 9, respectively. At a recirculation ratio of 9, the struvite content of the product was 80%. The percentage recovery of sand phosphate content was 6.91% higher, whereas that of ammonium was 3.9% higher, when compared to a recirculation ratio of 6. The higher ammonium recovery percentage indicated that more ammonium ions reacted to form the desired product [38]. Li reported that higher ammonium content can increase the purity of crystals [32].

At a recirculation ratio of 9, struvite along with few other crystals were formed, namely, MgF_2, newberryite, and fluoride. However, the struvite content was still the highest. Table 4 lists the composition and weight of the resulting products. The percentage of struvite crystals in the resulting product was 54%, with a recirculation ratio of 6. The amount of struvite produced was low; however, the number of impurity ions attached to the crystals was considerably smaller. This was due to the recirculation process, in which the formed nuclei react more quickly with other similar nuclei [39]. Therefore, competition exists between the impurity ions and mag-nesium, ammonium, and phosphate to form struvite [40].

In products of crystals, in addition to the main component - struvite, also all impurities that initially existed in wastewater appear in the form of hydroxides and other salts [13]. The crystals formed using the optimum velocity for each seed-material variable were analyzed for Mg, NH_4^+, and PO_4^{3-} contents using the wet analysis method. The molar ratio of $[NH^{4+}]:[PO_4^{3-}]:[Mg^{2+}]$ was not 1:1:1,
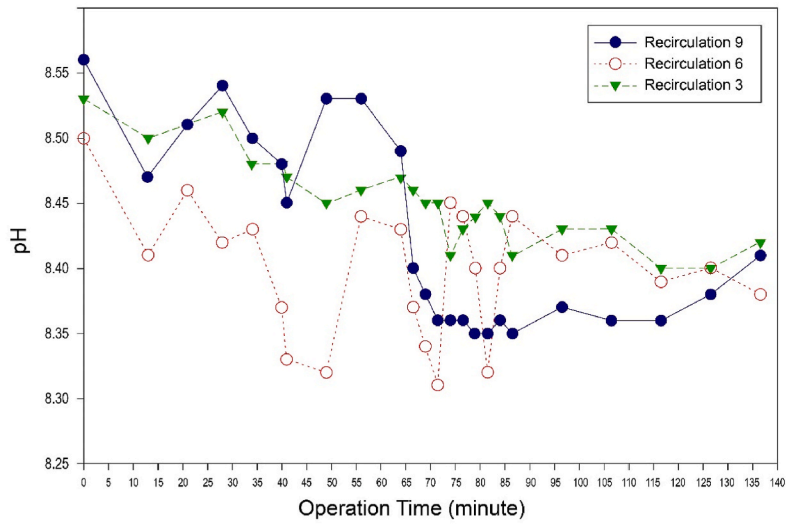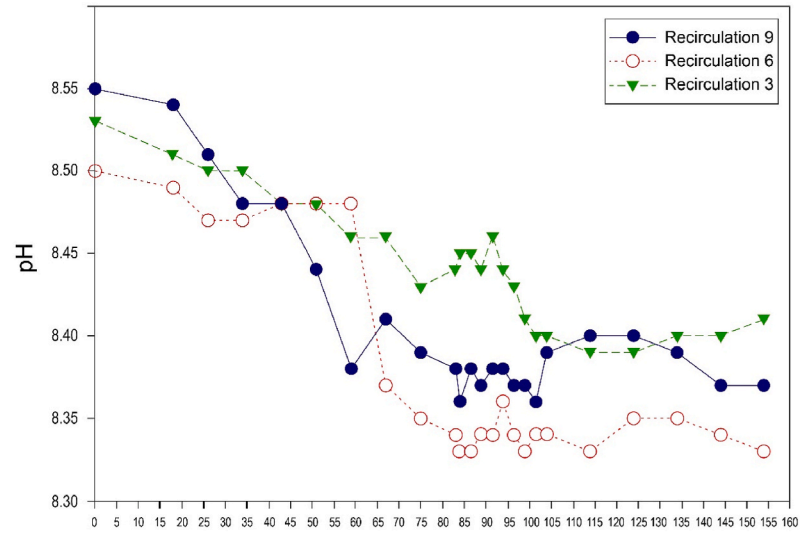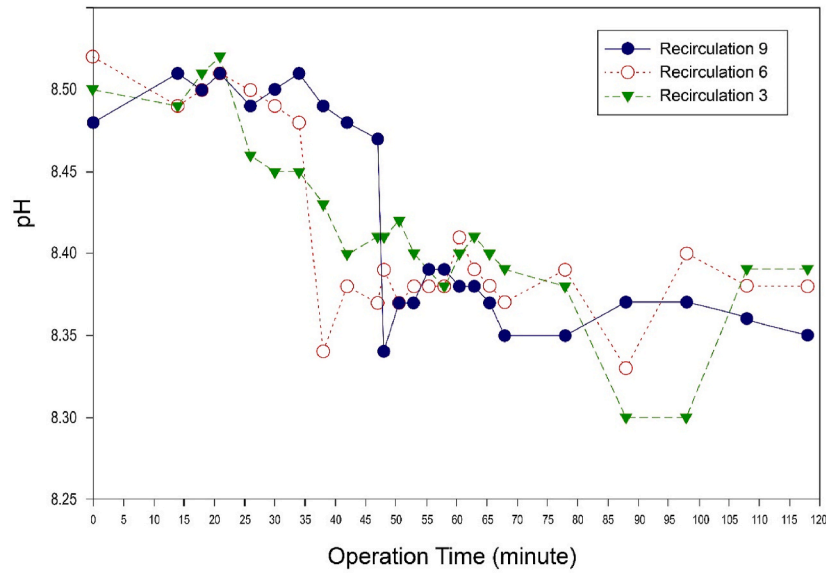
Fig. 2. Effect on pH with recirculation and hydraulic loading rates of 0.39 L/min **(A),** 0.59 L/min **(B),** 0.79 L/min **(C).**

Table 3
Effect of recirculation ratio and hydraulic loading rate on TSS removal.

No	Recirculation ratio	Hydraulic loading rate (L/min)	TSS (mg/L)		Percentage of TSS removal
			start	finish	
1	9	0.39	122.02	92.98	23.8%
2		0.59	122.01	92.07	24.5%
3		0.79	122.03	95.14	22.0%
4	6	0.39	123.00	96.00	22.0%
5		0.59	122.03	97.00	20.5%
6		0.79	101.84	88.94	12.7%
7	3	0.39	100.19	90.10	10.1%
8		0.59	100.10	89.95	10.1%
9		0.79	100.81	90.38	10.3%

which was similar to the ideal molar ratio of struvite. This was because the resulting product contained impurities formed during struvite crystallization [3]. The magnesium content was high because magnesium does not entirely react with struvite [41]. Subsequently, other compounds were formed. At a recirculation ratio of 9, the molar ratio $[NH^{4+}]:[PO_4^{3-}]:[Mg^{2+}]$ was close to 1:1:1, which was consistent with the XRD analysis results shown in Fig. 4(B), which shows these variations in struvite. However, several other crystals were formed in small amounts, namely $MgSiO_3$, CaF_2, bobierrite, magnesium phosphate, and newberryite.
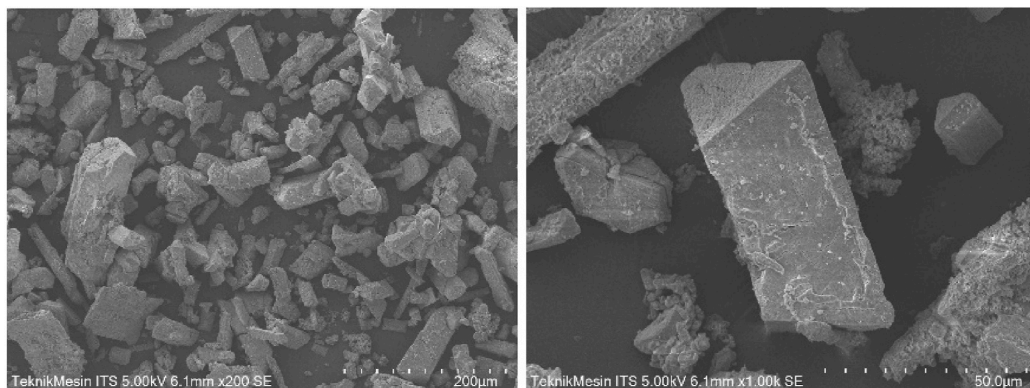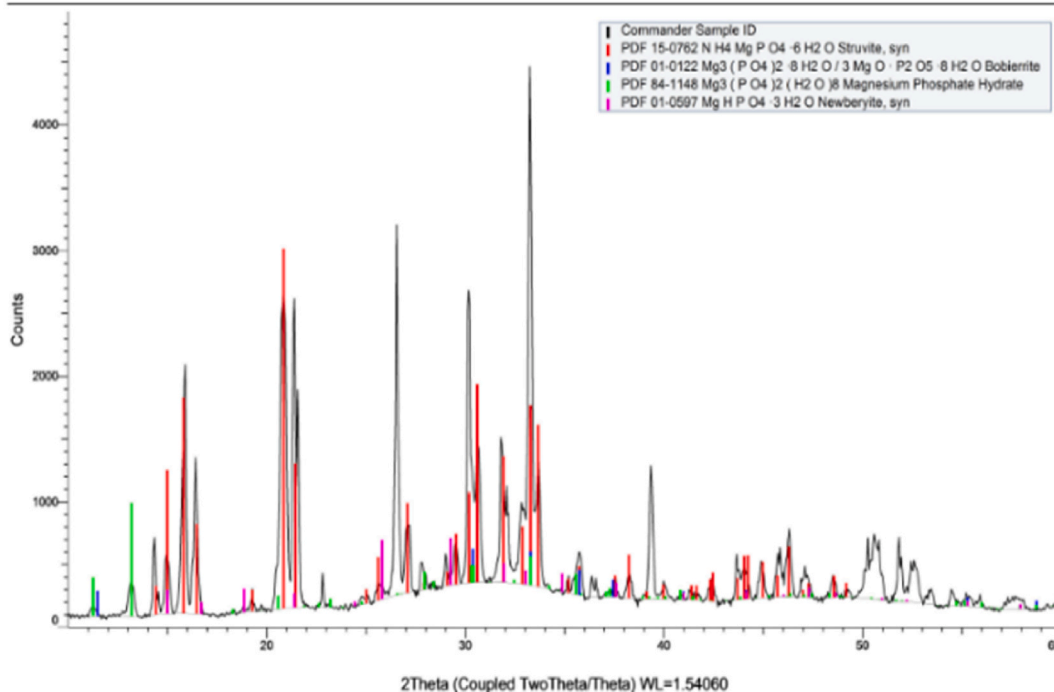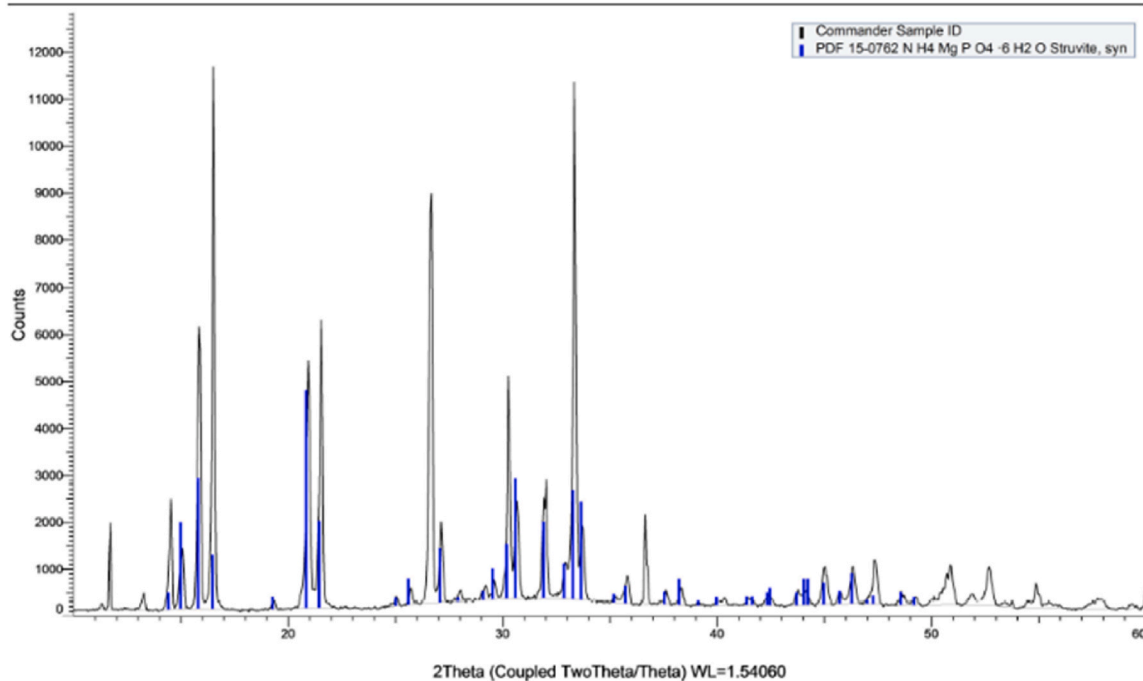

(A)
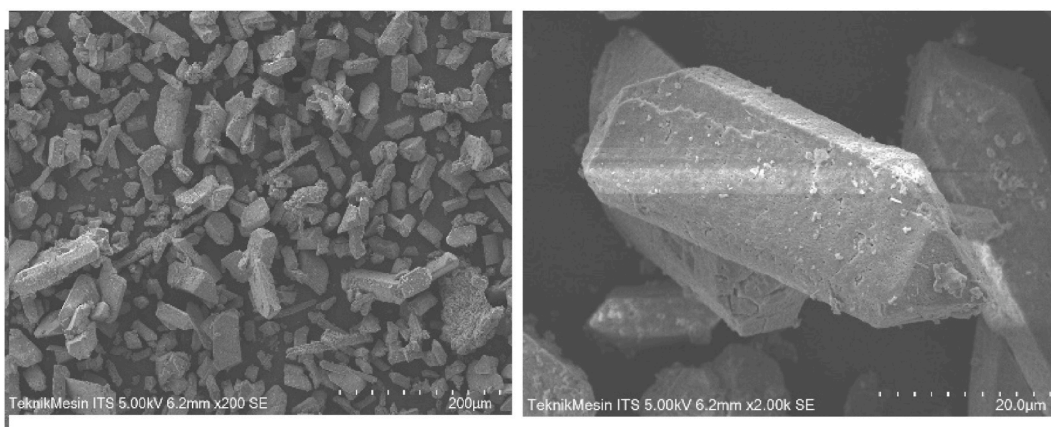
(B)

Fig. 3. SEM analysis results **(A)** considering a recirculation ratio of 9 and hydraulic loading rate of 0.39 L/min with 100 times magnification (left) and 1000 times magnification (right) and **(B)** considering a recirculation ratio of 6 and hydraulic loading rate 0.39 L/min with 100 times magnification (left) and 1000 times magnification (right).

(A)

(B)

Fig. 4. XRD analysis results **(A)** at a recirculation ratio of 6 with hydraulic loading rate of 0.39 L/min and **(B)** at a recirculation ratio of 9 with hydraulic loading rate of 0.39 L/min.

Table 4

Percentage and weight of product compounds.

No	Recirculation ratio	Crystals	Percentages	Total of product (g)	Weight (g)
1	9	*Struvite*	80%	1542	1233.60
2		MgF_2	13%		200.46
3		*Newberryite*	5%		77.10
4		*Fluorite*	2%		30.84
1	6	Struvite	54%	1032	557.28
2		$Mg_2(PO_2)_2$	12%		125.90
3		$MgSiO_2$	15%		156.86
4		Bobierrite	9%		91.85
5		Newberryite	8%		83.59
6		Fluorapatite	2%		16.51

5. Conclusion

The optimum recirculation ratio, which is an essential factor in fertilizer industry wastewater treatment, was 9. This recirculation ratio can result in a 55.71% reduction in the phosphate concentration and a 49.69% reduction in the ammonium concentration. The optimum hydraulic loading rate for this process was 0.39 L/min. Thus, a lower loading rate can result in a higher removal efficiency of phosphate and ammonium because of the longer detention time of the wastewater in the reactor. According to the SEM-EDX results, 80% of the crystals produced were composed of struvite. This study also found that better ammonium and phosphate recovery efficiencies can be achieved with a larger recirculation ratio and longer retention time for treated wastewater. Therefore, increasing the retention time can lead to higher recovery of nutrients from wastewater. Suggestions for future research can be made to automatically control the pH in the reactor so that the pH during the fluidization process remains at pH 8.5. Increasing the struvite content in wastewater can be done by using struvite as a seed material with a recirculation process. Fertilizer wastewater that has many impurities ions, so pre-treatment should be needed to remove these ions that inhibit the formation of ammonium phosphate recovery and the formation of struvite.

Author contribution statement

I Dewa Ayu Agung Warmadewanthi: Conceived and designed the experiments; Contributed reagents, materials, analysis tools or data; Wrote the paper. Nurani Ikhlas: Analyzed and interpreted the data; Wrote the paper. Febrianda Damayanti: Performed the experiments; Analyzed and interpreted the data.

Data availability statement

Data will be made available on request.

Declaration of competing interest

The authors declare that they have no known competing financial interests or personal relationships that could have appeared to influence the work reported in this paper.

Acknowledgements

References

[1] V.M. Bhandari, L.G. Sorokhaibam, V.V. Ranade, Industrial Wastewater Treatment for Fertilizer Industry—A Case Study, Desalination and Water Treatment, 2016, pp. 1–11, https://doi.org/10.1080/19443994.2016.1186399.

[2] N. Ikhlas, Removal of Ammonium and Phosphate from Fertilizer Industry Wastewater Using Struvite Precipitation Method, 2017.

[3] L.N. Affonso, J.L. Marques, V.V.C. Lima, J.O. Gonçalves, S.C. Barbosa, E.G. Primel, T.A.L. Burgo, G.L. Dotto, L.A.A. Pinto, T.R.S. Cadaval, Removal of fluoride from fertilizer industry effluent using carbon nanotubes stabilized in chitosan sponge, J. Hazard Mater. 388 (2020), 122042, https://doi.org/10.1016/j.jhazmat.2020.122042.

[4] S. Georg, A.T. Puari, M.P.G. Hanantyo, T. Sleutels, P. Kuntke, A. ter Heijne, C.J.N. Buisman, Low-energy ammonium recovery by a combined bio-electrochemical and electrochemical system, Chem. Eng. J. 454 (2023), 140196, https://doi.org/10.1016/j.cej.2022.140196.

[5] Y.-J. Shih, R.R.M. Abarca, M.D.G. de Luna, Y.-H. Huang, M.-C. Lu, Recovery of phosphorus from synthetic wastewaters by struvite crystallization in a fluidized-bed reactor: effects of pH, phosphate concentration and coexisting ions, Chemosphere 173 (2017) 466–473, https://doi.org/10.1016/j.chemosphere.2017.01.088.

[6] P. Cornel, C. Schaum, Phosphorus recovery from wastewater: needs, technologies and costs, Water Sci. Technol. : A Journal of the International Association on Water Pollution Research 59 (2009) 1069–1076, https://doi.org/10.2166/wst.2009.045.

[7] C.T. Reinhard, N.J. Planavsky, B.C. Gill, K. Ozaki, L.J. Robbins, T.W. Lyons, W.W. Fischer, C. Wang, D.B. Cole, K.O. Konhauser, Evolution of the global phosphorus cycle, Nature 541 (2017) 386–389, https://doi.org/10.1038/nature20772.

[8] H. Huang, J. Li, B. Li, D. Zhang, N. Zhao, S. Tang, Comparison of different K-struvite crystallization processes for simultaneous potassium and phosphate recovery from source-separated urine, Sci. Total Environ. 651 (2019) 787–795, https://doi.org/10.1016/j.scitotenv.2018.09.232.

[9] M. Alijani Galangashi, S.F. Masoumi Kojidi, A. Pendashteh, B. Abbasi Souraki, A.A. Mirroshandel, Removing iron, manganese and ammonium ions from water using greensand in fluidized bed process, J. Water Proc. Eng. 39 (2021), 101714, https://doi.org/10.1016/j.jwpe.2020.101714.

[10] Y. Leng, A. Soares, Microbial phosphorus removal and recovery by struvite biomineralisation in comparison to chemical struvite precipitation in municipal wastewater, J. Environ. Chem. Eng. 11 (2023), 109208, https://doi.org/10.1016/j.jece.2022.109208.

[11] D. Hikmawati, A. Bagastyo, I. Warmadewanthi, Electrodialytic recovery of ammonium and phosphate ions in fertilizer industry wastewater by using a continuous-flow reactor, J. Ecol. Eng. 20 (2019) 255–263, https://doi.org/10.12911/22998993/109461.

[12] W. Warmadewanthi, E.S. Pandebesie, W. Herumurti, A.Y. Bagastyo, M. Misbachul, Phosphate recovery from wastewater of fertiliser industries by using gypsum waste, Chemical Engineering Transactions 56 (2017) 1765–1770, https://doi.org/10.3303/CET1756295.

[13] A. Matynia, B. Wierzbowska, N. Hutnik, A. Mazienczuk, A. Kozik, K. Piotrowski, Separation of struvite from mineral fertilizer industry wastewater, Procedia Environmental Sciences 18 (2013) 766–775, https://doi.org/10.1016/j.proenv.2013.04.103.

[14] B. Li, I. Boiarkina, W. Yu, H.M. Huang, T. Munir, G.Q. Wang, B.R. Young, Phosphorous recovery through struvite crystallization: challenges for future design, Sci. Total Environ. 648 (2019) 1244–1256, https://doi.org/10.1016/j.scitotenv.2018.07.166.

[15] C. Zhang, K. Xu, J. Li, C. Wang, M. Zheng, Recovery of phosphorus and potassium from source-separated urine using a fluidized bed reactor: optimization operation and mechanism modeling, Ind. Eng. Chem. Res. 56 (2017) 3033–3039, https://doi.org/10.1021/acs.iecr.6b04819.

[16] M. Ronteltap, M. Maurer, R. Hausherr, W. Gujer, Struvite precipitation from urine – influencing factors on particle size, Water Res. 44 (2010) 2038–2046, https://doi.org/10.1016/j.watres.2009.12.015.

[17] S. Shim, S. Won, A. Reza, S. Kim, N. Ahmed, C. Ra, Design and optimization of fluidized bed reactor operating conditions for struvite recovery process from swine wastewater, Processes 8 (2020) 422, https://doi.org/10.3390/pr8040422.

[18] A. Warmadewanthi, N. Rodlia, E.S. Ikhlas, A.Y. Pandebesie, W. Bagastyo, Herumurti, The effect of mixing rate on struvite recovery from the fertilizer industry, IOP Conf. Ser. Earth Environ. Sci. 506 (2020), 012013, https://doi.org/10.1088/1755-1315/506/1/012013.

[19] S.F. Valle, A.S. Giroto, V. Dombinov, A.A. Robles-Aguilar, N.D. Jablonowski, C. Ribeiro, Struvite-based composites for slow-release fertilization: a case study in sand, Sci. Rep. 12 (2022), 14176, https://doi.org/10.1038/s41598-022-18214-8.

[20] M. Alruqi, P. Sharma, Biomethane production from the mixture of sugarcane vinasse, solid waste and spent tea waste: a bayesian approach for hyperparameter optimization for Gaussian process regression, Fermentation 9 (2023) 120, https://doi.org/10.3390/fermentation9020120.

[21] M.I.H. Bhuiyan, D.S. Mavinic, F.A. Koch, Phosphorus recovery from wastewater through struvite formation in fluidized bed reactors: a sustainable approach, Water Sci. Technol. 57 (2008) 175–181, https://doi.org/10.2166/wst.2008.002.

[22] Y. Warmadewanthi, Fitri Rajabi Bachtiar, Study of struvite crystallization from fertilizer industry wastewater by using fluidized bed reactor, MATEC Web Conf 276 (2019), 06006, https://doi.org/10.1051/matecconf/201927606006.

[23] Z.-G. Liu, X.-B. Min, F. Feng, X. Tang, W.-C. Li, C. Peng, T.-Y. Gao, X.-L. Chai, C.-J. Tang, Development and simulation of a struvite crystallization fluidized bed reactor with enhanced external recirculation for phosphorous and ammonium recovery, Sci. Total Environ. 760 (2021), 144311, https://doi.org/10.1016/j.scitotenv.2020.144311.

[24] W.R. Abma, W. Driessen, R. Haarhuis, M.C.M. van Loosdrecht, Upgrading of sewage treatment plant by sustainable and cost-effective separate treatment of industrial wastewater, Water Sci. Technol. 61 (2010) 1715–1722, https://doi.org/10.2166/wst.2010.977.

[25] Y. Suleiman, Design and fabrication of fluidized-bed reactor, International Journal of Engineering and Computer Science 2 (2013) 1595–1605.

[26] X. Ye, Z.-L. Ye, Y. Lou, S. Pan, X. Wang, M.K. Wang, S. Chen, A comprehensive understanding of saturation index and upflow velocity in a pilot-scale fluidized bed reactor for struvite recovery from swine wastewater, Powder Technol. 295 (2016) 16–26, https://doi.org/10.1016/j.powtec.2016.03.022.

[27] K.S. Le Corre, E. Valsami-Jones, P. Hobbs, B. Jefferson, S.A. Parsons, Agglomeration of struvite crystals, Water Res. 41 (2007) 419–425, https://doi.org/10.1016/j.watres.2006.10.025.

[28] M.M. Seckler, Crystallization in fluidized bed reactors: from fundamental knowledge to full-scale applications, Crystals 12 (2022) 1541, https://doi.org/10.3390/cryst12111541.

[29] H. Huang, Y. Chen, Y. Jiang, L. Ding, Treatment of swine wastewater combined with MgO-saponification wastewater by struvite precipitation technology, Chem. Eng. J. 254 (2014) 418–425, https://doi.org/10.1016/j.cej.2014.05.054.

[30] R. Xiao, Y. Wei, D. An, D. Li, X. Ta, Y. Wu, Q. Ren, A review on the research status and development trend of equipment in water treatment processes of recirculating aquaculture systems, Rev. Aquacult. 11 (2019) 863–895, https://doi.org/10.1111/raq.12270.

[31] E. Tarragó, S. Puig, M. Ruscalleda, M.D. Balaguer, J. Colprim, Controlling struvite particles' size using the up-flow velocity, Chem. Eng. J. 302 (2016) 819–827, https://doi.org/10.1016/j.cej.2016.06.036.

[32] C.W. Liu, Y. Sung, B.C. Chen, H.Y. Lai, Effects of nitrogen fertilizers on the growth and nitrate content of lettuce (Lactuca sativa L.), Int. J. Environ. Res. Publ. Health 11 (2014) 4427–4440, https://doi.org/10.3390/ijerph110404427.

[33] M.D.G. de Luna, L.H.S. Paulino, C.M. Futalan, M.C. Lu, Recovery of zinc granules from synthetic electroplating wastewater using fluidized-bed homogeneous crystallization process, Int. J. Environ. Sci. Technol. 17 (2020) 129–142, https://doi.org/10.1007/s13762-019-02439-8.

[34] N. Krishnamoorthy, Y. Unpaprom, R. Ramaraj, G.P. Maniam, N. Govindan, T. Arunachalam, B. Paramasivan, Recent advances and future prospects of electrochemical processes for microalgae harvesting, J. Environ. Chem. Eng. 9 (2021), https://doi.org/10.1016/j.jece.2021.105875.

[35] N. Hutnik, A. Kozik, A. Mazienczuk, K. Piotrowski, B. Wierzbowska, A. Matynia, Phosphates (V) recovery from phosphorus mineral fertilizers industry wastewater by continuous struvite reaction crystallization process, Water Res. 47 (2013) 3635–3643, https://doi.org/10.1016/j.watres.2013.04.026.

[36] V.-G. Le, D.-V.N. Vo, N.-H. Nguyen, Y.-J. Shih, C.-T. Vu, C.-H. Liao, Y.-H. Huang, Struvite recovery from swine wastewater using fluidized-bed homogeneous granulation process, J. Environ. Chem. Eng. 9 (2021), 105019, https://doi.org/10.1016/j.jece.2020.105019.

[37] C.-C. Su, L.D. Dulfo, M.L.P. Dalida, M.-C. Lu, Magnesium phosphate crystallization in a fluidized-bed reactor: effects of pH, Mg:P molar ratio and seed, Sep. Purif. Technol. 125 (2014) 90–96, https://doi.org/10.1016/j.seppur.2014.01.019.

[38] L. Hu, J. Yu, H. Luo, H. Wang, P. Xu, Y. Zhang, Simultaneous recovery of ammonium, potassium and magnesium from produced water by struvite precipitation, Chem. Eng. J. 382 (2020), 123001, https://doi.org/10.1016/j.cej.2019.123001.

[39] K.A.A. Tiangco, M.D.G. de Luna, A.C. Vilando, M.-C. Lu, Removal and recovery of calcium from aqueous solutions by fluidized-bed homogeneous crystallization, Process Saf. Environ. Protect. 128 (2019) 307–315, https://doi.org/10.1016/j.psep.2019.06.007.

[40] N.Y. Acelas, E. Flórez, D. López, Phosphorus recovery through struvite precipitation from wastewater: effect of the competitive ions, Desalination Water Treat. 54 (2015) 2468–2479, https://doi.org/10.1080/19443994.2014.902337.

[41] S. Li, W. Zeng, H. Xu, Z. Jia, Y. Peng, Performance investigation of struvite high-efficiency precipitation from wastewater using silicon-doped magnesium oxide, Environ. Sci. Pollut. Res. 27 (2020) 15463–15474, https://doi.org/10.1007/s11356-019-07589-3.

[42] APHA, Standard Methods for the Examination of Water and Wastewater, 23rd ed., 2017. Washington.